Proceedings of the
46th IEEE Conference on Decision and Control
New Orleans, LA, USA, Dec. 12-14, 2007

Diversified Redundancy in the Measurement of Euler Angles Using Accelerometers and Magnetometers

Chirag Jagadish and Bor-Chin Chang, *Member, IEEE*
Drexel University, Philadelphia, Pennsylvania, 19104

***Abstract* – Euler angle determination plays an important role in control of aerial vehicles. Euler angles can be determined based on the measurements of the projections of earth magnetic field and gravity on the three body axes of the vehicle. The proposed approach utilizes seven methods to compute the Euler angles and each of these methods employs a different subset of the six measurements. The capability of computing the Euler angles in multiple ways provides a diversified redundancy required for fault tolerance. This diversified redundancy can be also used to separate the desired measurement from extraneous interferences and to identify sensor failures.**

***Keywords* –** Euler angles, Accelerometers, Magnetometers, Fault tolerant sensing, Diversified redundancy.

I. Introduction

Euler angles θ, ϕ, and ψ (pitch, roll, and yaw angles) are essential in control of aerial vehicles. In the conventional aircraft, Euler angles are obtained through the use of IMUs (inertial measurement units) consisting of sensors like mechanical gyroscopes, accelerometers and magnetometers. These IMUs usually are bulky and costly, and not suitable for relatively cheaper applications like flying munitions [1, 2] and small organic UAVs (unmanned aerial vehicles). With rapid advances in sensor and embedded computer technology, smaller, lighter, and less expensive sensors like the AMR (anisotropic magneto resistive) magnetometers [2, 3] and MEMS (Micro Electro Mechanical Systems) accelerometers [4, 5] have started to gain popularity. These components are usually available as three-axis packages smaller than 0.1 cubic inch. These are being used to construct the attitude measuring devices for smaller vehicles [6, 7].

The accelerometers and magnetometers measure the projections of acceleration due to gravity and the magnetic field of the earth on the aerial vehicle. These projections are utilized to compute the angular position of the vehicle, which is described by Euler angles.

Euler angles [8-10] are defined based on a particular rotation sequence called as aerospace or yaw-pitch-roll rotation sequence. An equation based on this rotation sequence provides a way of computing the Euler angles using three out of the six available measurements. If these three measurements are accurate and reliable, then the other three sensors become redundant. However, extraneous field interferences or failure on one or more of these critical sensors can go undetected and cause the sensor system to fail.

The fault tolerant sensor issues have been studied extensively [11, 12]. One is to employ duplicate sensors [13]. This solution overcomes the problems related to component failure but cannot resolve those caused by extraneous fields since the extraneous field would affect both the main sensor and all its duplicates in similar fashion. Multiple sensors of different types are also used to provide redundancy for sensor health monitoring [14]. More sensors can solve the problem but as vehicles become smaller, the pay load, space and power constraints may limit the use of multiple sensors. Kalman estimation has also been proposed [14-16] to estimate the states of a system in cases related to sensor failures. To use this approach, the system dynamics and the stochastic characteristics of the interferences and noises are assumed given.

A solution to the fault tolerant sensing issue proposed in this paper is in finding alternative computation methods for Euler angles. The solution has to be such that each method uses different rotation-sequence matrices [17] and require different subsets of sensor data among the six accelerometer and magnetometer measurements available. The ability to use different subsets of sensor measurements would improve fault tolerance in the sensor system. Since each of the sensor axes is oriented in mutually perpendicular directions, an extraneous field would not cause similar type of interference in all of them at the same time. This fact creates diversified redundancy in the sensors. The proposed approach can identify healthy sensors, detect faults, and even separate the extraneous interference signal from the intended measurement. Computing the extraneous interference signals sometimes may be of interest, for example, when they are acceleration caused by the motion of the vehicle.

An important point to note is that Euler angles are defined according to the aerospace sequence. It is required as a part of the proposed approach to compute Euler angles from all the possible rotation sequence matrices. If a different rotation sequence is used, the rotation angles obtained are different from the standard Euler angles. The angle obtained then has to be converted to the standard Euler angles. Although the proposed approach requires more computation, today's embedded computing power has made it possible to implement it in real world applications.

There are issues related to singularity points in computation based on rotation matrices and inverse trigonometric functions. The issues can be addressed using the concept of Quaternions [18-20].

Chirag Jagadish, Graduate student, Dept. of Mechanical Engineering, Drexel University, Philadelphia, PA 19104. cj362@drexel.edu
Bor-Chin Chang, Professor, Dept. of Mechanical Engineering, Drexel University, Philadelphia, PA 19104. bchang@coe.drexel.edu

1-4244-1498-9/07/$25.00 ©2007 IEEE.

The remainder of the paper is organized as follows. Section II consists of the preliminary knowledge required for later sections. Section III presents the proposed approach of using the diversified redundancy effectively to improve the fault tolerance of the sensor system. Section IV gives a numerical example to demonstrate the concepts. Section V is the conclusion.

II. PRELIMINARY

The sensors used in this application are three-axis accelerometers and three-axis magnetometers. The sensors mounted on the axes measure the projection of these fields (acceleration or magnetic field) in each direction of the three dimensional space. The fields of interest in this application are the gravity and magnetic field of the earth. These fields are assumed given and can be utilized as references for measuring the angular position of the vehicle.

The angular position is represented as a combination of three angles θ, ϕ, and ψ called Euler angles. Each of these angles represents the rotation of the vehicle with respect to the *y, x* and *z* axes of the body respectively. Fig. 1 shows the relation between the axes and the rotation angles.

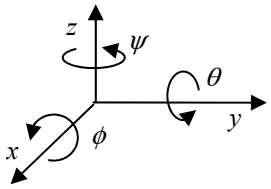

Fig. 1. Relation between rotation angles and axes of rotation.

Calculating Euler angles using rotation matrix method is simplified if initial vectors of acceleration and magnetic field are in the form $\begin{bmatrix} a_x & a_y & a_z \end{bmatrix} = \begin{bmatrix} 0 & 0 & 1 \end{bmatrix}$ and $\begin{bmatrix} m_x & m_y & m_z \end{bmatrix} = \begin{bmatrix} \cos\alpha & 0 & \sin\alpha \end{bmatrix}$ respectively where α is the inclination angle of the earth magnetic field [21]. With the initial vectors shown as above, the earth frame *XYZ* or the initial position of the vehicle is oriented so that its *xz* plane is vertical and coincides with the plane of the magnetic field of the earth and *xy* plane is horizontal and parallel to the surface of the earth. The sensors are mounted on the *xyz* axes of the vehicle, which form the body frame *xyz* as shown in Fig. 2.

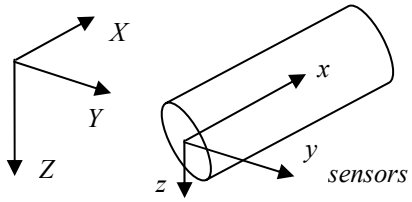

Fig. 2. Orientation of accelerometer & magnetometer in body.

Euler angles can be determined by the above initial vectors and the final vectors that measure the projection of the earth gravity and magnetic fields on the vehicle axes at the final position. Euler angles are defined based on a particular rotation sequence: yaw-pitch-roll sequence or the aerospace sequence.

Aerospace sequence or Yaw-Pitch-Roll sequence

This method utilizes the aerospace rotation sequence matrix [22, 23]. The calculations used to obtain the Euler angles are shown in Eq. (2) below.

$$\begin{bmatrix} a_x \\ a_y \\ a_z \end{bmatrix} = \begin{bmatrix} c\theta c\psi & c\theta s\psi & -s\theta \\ s\phi s\theta c\psi - c\phi s\psi & s\phi s\theta s\psi + c\phi c\psi & s\phi c\theta \\ c\phi s\theta c\psi + s\phi s\psi & c\phi s\theta s\psi - s\phi c\psi & c\phi c\theta \end{bmatrix} \begin{bmatrix} 0 \\ 0 \\ 1 \end{bmatrix}$$
$$\begin{bmatrix} m_x \\ m_y \\ m_z \end{bmatrix} = \begin{bmatrix} c\theta c\psi & c\theta s\psi & -s\theta \\ s\phi s\theta c\psi - c\phi s\psi & s\phi s\theta s\psi + c\phi c\psi & s\phi c\theta \\ c\phi s\theta c\psi + s\phi s\psi & c\phi s\theta s\psi - s\phi c\psi & c\phi c\theta \end{bmatrix} \begin{bmatrix} c\alpha \\ 0 \\ s\alpha \end{bmatrix} \quad (1)$$

From Eq. (1), the Euler angles can be calculated through the equations

$$\theta = -\sin^{-1}(a_x)$$
$$\phi = \sin^{-1}(a_y / \cos\theta) \quad (2)$$
$$\psi = \cos^{-1}([m_x + \sin\theta\sin\alpha]/[\cos\theta\cos\alpha])$$

It is to be noted that this method depends on the use of sensor axes a_x, a_y and m_x. Any external fields influencing the measurement of these sensors or a failure of one of these sensors would result in erroneous measurement results. Other rotation sequence formulations for calculating Euler angles are presented in the following section.

III. MAIN RESULT

In this section, we will present alternative formulations to calculate the Euler angles using different rotation sequence matrices [17] and utilize them to provide diversified redundancy required for fault tolerance. The redundancy also allows us to extract the extraneous field, like the acceleration due to the motion of vehicle or magnetic field caused by electric wires.

A. Alternative Euler angle calculation methods

The methods of calculating Euler angles using alternative rotation matrix formulations are demonstrated in this section. The rotation angles computed based on these new computation methods do not equal to, but can be converted to the standard Euler angles. The equations for computing the rotation angles and the equations to convert them to standard Euler angles are shown in the following.

1) Aerospace sequence (alternative formulation)

Using the aerospace sequence rotation matrix, an alternate formulation to find the Euler angles is shown below.

$$\phi = \tan^{-1}(a_y / a_z)$$
$$\theta = \cos^{-1}(a_y / \sin\phi) \quad (3a)$$
$$\psi = \sin^{-1}\left([A(m_z - D) - E(m_y - C)]/(BE + AF)\right)$$

where

$$A=(\sin\phi)(\sin\theta)(\cos\alpha),\quad B=(\cos\phi)(\cos\alpha)$$
$$C=(\sin\phi)(\cos\theta)(\sin\alpha),\quad D=(\cos\phi)(\cos\theta)(\sin\alpha) \quad (3b)$$
$$E=(\cos\phi)(\sin\theta)(\cos\alpha),\quad F=(\sin\phi)(\cos\alpha)$$

Eq. (3) shows that this method requires the use of the measurements a_y, a_z, m_y and m_z. Since it uses the same rotation sequence and only the calculation procedure is different, the angles produced are standard Euler angles.

2) Roll-Pitch-Yaw sequence

This method uses the rotation matrix shown in Eq. (4) below. Based on this rotation matrix, the rotation angles θ_1, ϕ_1 and ψ_1 are computed using Eq. (5).

$$\begin{bmatrix}a_x\\a_y\\a_z\end{bmatrix}=\begin{bmatrix}\mathrm{c}\psi_1\,\mathrm{c}\theta_1 & s\psi_1c\phi_1+c\psi_1s\theta_1s\phi_1 & s\psi_1s\phi_1-c\psi_1s\theta_1c\phi_1\\ -\mathrm{s}\psi_1\,\mathrm{c}\theta_1 & c\psi_1c\phi_1-s\psi_1s\theta_1s\phi_1 & c\psi_1s\phi_1+s\psi_1s\theta_1c\phi_1\\ \mathrm{s}\theta_1 & -c\theta_1s\phi_1 & c\theta_1c\phi_1\end{bmatrix}\begin{bmatrix}0\\0\\1\end{bmatrix}$$
$$\begin{bmatrix}m_x\\m_y\\m_z\end{bmatrix}=\begin{bmatrix}\mathrm{c}\psi_1\,\mathrm{c}\theta_1 & s\psi_1c\phi_1+c\psi_1s\theta_1s\phi_1 & s\psi_1s\phi_1-c\psi_1s\theta_1c\phi_1\\ -\mathrm{s}\psi_1\,\mathrm{c}\theta_1 & c\psi_1c\phi_1-s\psi_1s\theta_1s\phi_1 & c\psi_1s\phi_1+s\psi_1s\theta_1c\phi_1\\ \mathrm{s}\theta_1 & -c\theta_1s\phi_1 & c\theta_1c\phi_1\end{bmatrix}\begin{bmatrix}\mathrm{c}\alpha\\0\\\mathrm{s}\alpha\end{bmatrix} \quad (4)$$

$$\theta_1=\sin^{-1}\left([m_z-a_z\sin\alpha]/\cos\alpha\right)$$
$$\phi_1=\cos^{-1}\left(a_z/\cos\theta_1\right) \quad (5a)$$
$$\psi_1=\sin^{-1}\left([Bm_x-Am_y]/[A^2+B^2]\right)$$

where

$$A=\cos\theta_1\cos\alpha-\sin\theta_1\cos\phi_1\sin\alpha$$
$$B=\sin\phi_1\sin\alpha \quad (5b)$$

The rotation angles θ_1, ϕ_1 and ψ_1 obtained from Eq. (5) are converted to the standard Euler angles using Eq. (6) below.

$$\theta=\sin^{-1}\left(\cos\phi_1\sin\theta_1\cos\psi_1-\sin\phi_1\sin\psi_1\right)$$
$$\phi=\cos^{-1}\left(\cos\theta_1\cos\phi_1/\cos\theta\right) \quad (6)$$
$$\psi=\cos^{-1}\left(\cos\theta_1\cos\psi_1/\cos\theta\right)$$

Thus, it is seen that standard Euler angles can be computed using the measurements a_z, m_x, m_y and m_z,.

3) Yaw-Roll-Pitch sequence

Similarly the rotation angles can be obtained using the yaw-roll-pitch sequence rotation matrix and can be converted to standard Euler angles using the Eqs. (7) and (8) shown below.

$$\phi_2=\sin^{-1}\left(a_y\right)$$
$$\theta_2=\cos^{-1}\left(a_z/\cos\phi_2\right) \quad (7)$$
$$\psi_2=\sin^{-1}\left([m_y-\sin\phi_2\sin\alpha]/[\cos\phi_2\cos\alpha]\right)$$
$$\theta=\sin^{-1}\left(\cos\phi_2\sin\theta_2\right)$$
$$\phi=\sin^{-1}\left(\sin\phi_2/\cos\theta\right) \quad (8)$$
$$\psi=\cos^{-1}\left([\cos\psi_2\cos\theta_2-\sin\psi_2\sin\theta_2\sin\phi_2]/\cos\theta\right)$$

As seen from the equations above, this method uses the measurements a_y, a_z and m_y.

4) Roll-Yaw-Pitch sequence

This rotation sequence method uses the measurements a_x, a_y, a_z and m_y. The equations used to calculate the Euler angles are shown as follows.

$$\psi_3=\sin^{-1}\left([a_y\sin\alpha-m_y]/\cos\alpha\right)$$
$$\phi_3=\sin^{-1}\left(a_y/\cos\psi_3\right) \quad (9a)$$
$$\theta_3=\sin^{-1}\left([Aa_z-Ba_x]/[A^2+B^2]\right)$$

where

$$A=\sin\phi_3\sin\psi_3,\quad B=\cos\phi_3 \quad (9b)$$

Therefore,

$$\theta=\sin^{-1}\left(\cos\phi_3\sin\theta_3-\cos\theta_3\sin\phi_3\sin\psi_3\right)$$
$$\phi=\sin^{-1}\left([\cos\psi_3\sin\phi_3]/\cos\theta\right)$$
$$\psi=\cos^{-1}\left([\cos\theta_3\cos\psi_3]/\cos\theta\right)$$
(10)

5) Pitch-Roll-Yaw sequence

The equations to obtain the Euler angles from this rotation sequence require the measurements a_x, a_y, a_z and m_z. The equations used are shown below.

$$\theta_4=\tan^{-1}\left([m_z-a_z\sin\alpha]/[a_z\cos\alpha]\right)$$
$$\phi_4=\cos^{-1}\left(a_z/\cos\theta_4\right) \quad (11a)$$
$$\psi_4=\sin^{-1}\left([Aa_x+Ba_y]/[A^2+B^2]\right)$$

where

$$A=\cos\theta_4\sin\phi_4,\quad B=\sin\theta_4 \quad (11b)$$

Therefore,

$$\theta=\sin^{-1}\left(\cos\psi_4\sin\theta_4-\cos\theta_4\sin\phi_4\sin\psi_4\right)$$
$$\phi=\cos^{-1}\left([\cos\theta_4\cos\phi_4]/\cos\theta\right) \quad (12)$$
$$\psi=\sin^{-1}\left([\sin\psi_4\cos\phi_4]/\cos\theta\right)$$

6) Pitch-Yaw-Roll sequence

This method requires knowledge of a_x, m_x, m_y and m_z . The equations used are shown in the following.

$$\theta_5=\tan^{-1}\left([-a_x\cos\alpha]/[m_x-a_x\sin\alpha]\right)$$
$$\psi_5=\cos^{-1}\left(-a_x/\sin\theta\right) \quad (13a)$$
$$\phi_5=\cos^{-1}\left([Am_y+Bm_z]/[A^2+B^2]\right)$$

where

$$A=\sin\psi_5\sin\theta_5\sin\alpha-\sin\psi_5\cos\theta_5\cos\alpha$$
$$B=\sin\theta_5\cos\alpha+\cos\theta_5\sin\alpha \quad (13b)$$

Therefore,

$$\theta = \sin^{-1}\left(\cos\psi_5 \sin\theta_5\right)$$
$$\phi = \sin^{-1}\left([\sin\psi_5 \sin\theta_5 \cos\phi_5 + \cos\theta_5 \sin\phi_5]/\cos\theta\right) \quad (14)$$
$$\psi = \sin^{-1}\left(\sin\psi_5 / \cos\theta\right)$$

The different sets of sensor measurement data required for each method are tabulated in Table 1. From this table, it can be seen that there exists redundancy in the sensors used. This diversified redundancy can be utilized effectively for health monitoring of the sensors and separation of extraneous fields from earth gravity and magnetic field.

TABLE 1
ROTATION SEQUENCES AND THE DATA USED FOR EACH METHOD

	a_x	a_y	a_z	m_x	m_y	m_z
YPR	X	X		X		
YPR$_{alternat}$		X	X		X	X
RPY			X	X	X	X
YRP		X	X		X	
RYP	X	X	X		X	
PRY	X	X	X			X
PYR	X			X	X	X

X represents the use of the particular data towards calculation of Euler angles for the given method.

B. Extraneous field determination

For Euler angles determination, the accelerometers and magnetometers are to measure the projection of earth gravity and magnetic field in the three mutually perpendicular directions. Presence of extraneous acceleration or magnetic fields in any of these directions contaminates the sensor measurements. It should be noted that the extraneous field will affect the sensors in different ways. For example, it can be seen from Table 1 that any change in the measurement of acceleration a_x has no affect on the calculation of Euler angles using YPR$_{alternate}$, RPY and YRP sequence methods. But it will affect the calculations in different ways for YPR, RYP, PRY and PYR sequence methods. Knowing that some of the methods remain unaffected by an extraneous field and some of them are affected in particular ways, we can compute the extraneous field itself. The equations required for calculating extraneous acceleration fields a_x, a_y and a_z are shown in the following.

1) Extraneous acceleration in x direction

An extraneous acceleration in x direction affects the calculation of Euler angle in the methods involving YPR, RYP, PRY and PYR rotation sequences. In the case of YPR sequence, the measurement a_x is used in calculating the pitch angle θ as shown in Eq. (2). An extraneous acceleration in the x direction, e_x, causes the calculated pitch angle to be affected. The new equation can be written as below.

$$\hat{\theta} = -\sin^{-1}\left(a_x + e_x\right) \quad (15)$$

The correct pitch angle θ can be calculated using the methods which remain unaffected by the extraneous acceleration e_x , i.e. YPR$_{alternate}$, RPY and YRP. The pitch angle resulting from one of these methods is the uncontaminated Euler angle representing the pitch of the body. Therefore using this in Eq. (2), we obtain

$$\sin\theta = -a_x \quad (16)$$

Therefore the value of external acceleration e_x can be obtained by combining Eq. (15) and Eq.(16) as follows.

$$e_x = \sin\theta - \sin\hat{\theta} \quad (17)$$

2) Body accelerating in the y direction

Acceleration in the y direction can be determined similarly. The Euler angle calculated form the YRP sequence is contaminated by the extraneous acceleration in the y direction while the Euler angle calculated from the RPY or PYR rotation sequence method remains unaffected. It is seen from Eq. (7) that roll angle is modified by the extraneous acceleration in the y direction - e_y. The new angle that results is $\hat{\phi}_{yrp}$.

$$\hat{\phi}_{yrp} = \sin^{-1}\left(a_y + e_y\right) \quad (18)$$

The correct roll angle ϕ which is devoid of the effect of e_y can be obtained from the results of RPY sequence calculation. But the result of RPY calculation is the standard Euler angles ϕ and θ . These angles are converted to the YRP equivalent rotation angle using the following equation.

$$\phi_{yrp} = \sin^{-1}\left(\sin\phi\cos\theta\right) \quad (19)$$

Therefore Eq. (7) can be written as

$$\phi_{yrp} = \sin^{-1}\left(a_y\right) \quad (20)$$

Eqs. (18) and (20) can be combined to obtain the value of e_y as shown below.

$$\begin{aligned} e_y &= \sin\left(\hat{\phi}_{yrp}\right) - \sin\left(\phi_{yrp}\right) \\ &= \sin\left(\hat{\phi}_{yrp}\right) - \sin\phi\cos\theta \end{aligned} \quad (21)$$

3) Body accelerating in z direction

Similar to the above cases the extraneous acceleration in the z direction - e_z can be obtained using the acceleration contaminated angle $\hat{\phi}$ obtained from the YPR$_{alternate}$ sequence and the angle ϕ obtained from the PYR or the YPR sequence. Eq. (22) below shows the calculations required.

$$\begin{aligned} &\tan\hat{\phi} = a_y/(a_z + e_z), \quad \tan\phi = a_y/a_z \\ &\Rightarrow \quad e_z = (a_y/\tan\hat{\phi}) - (a_y/\tan\phi) \end{aligned} \quad (22)$$

A numerical example showing the extraction of the extraneous acceleration will be given in the next section. Similar methods can also be applied to calculate the extraneous magnetic fields in the x, y or z directions.

C. Detection of failed or contaminated sensors

If we know a sensor is experiencing extraneous

acceleration, a method can be devised to separate the extraneous field from the earth gravity. An algorithm is proposed in this section to detect if a sensor is contaminated with an extraneous acceleration or if the sensor has failed.

It is seen from Eqs. (1) to (14), and from Table 1 that different methods of calculating Euler angles utilize different sets of data. Provided that all the sensors are in good health and none of them are affected by any external fields, all seven methods will produce the same result. If an individual sensor axis fails or is contaminated, the results produced using this sensor will be inconsistent with those not affected by the contaminated sensor.

As an example, if the sensor axis a_x is contaminated, the Euler angles calculated using YPR, RYP, PRY and PYR methods are affected by this, but the other methods like $\text{YPR}_{\text{alternate}}$, RPY and YRP continue to produce correct Euler angle results since they do not use the value of a_x in the calculation. They are also consistent with each other. It is also of importance to note that the equations affected by the failure or external field are all affected in different ways and the results produced by them after the failure would be different from each other.

Similar is the case with sensor measuring acceleration in the y direction, i.e., a_y. Rotation sequences RPY and PYR will remain unaffected by a failure of sensor measuring a_y and produce correct and consistent results. All the other sequences are affected in different ways, and thus they produce inconsistent results.

Similar cases can be found for all the other sensor axes a_z, m_x, m_y and m_z , where, there are certain methods which produce consistent results and those which produce inconsistent results. The consistent results imply that they are correct, while the inconsistent results apparently are incorrect. This fact helps in identifying the failed and the functioning sensors. It also helps in filtering out the effect of the failure, i.e., it requires only two consistent results out of seven to produce the correct Euler angles. Thus the failure can not only be identified systematically but the effect of failure can be annulled in the Euler angle calculation procedure.

A numerical simulation is shown in the next section to illustrate this concept.

IV. Numerical Example

A simple simulation is presented to demonstrate the above concept. In this experiment, we consider a case where all the sensors are considered to be working perfectly and the vehicle is not experiencing any extraneous acceleration other than from the gravity of earth. Its angular position is considered to be such that it can be described by standard Euler angles $\theta = 45^o$, $\phi = 30^o$ and $\psi = 60^o$. The measurements, which are obtained at the accelerometer and magnetometer axes, are shown below.

$$a_x = -0.7071 \pm 0.01 \qquad m_x = -0.4356 \pm 0.01$$
$$a_y = 0.3536 \pm 0.01 \qquad m_y = 0.0196 \pm 0.01$$
$$a_z = 0.6124 \pm 0.01 \qquad m_z = 0.8999 \pm .01$$

The Euler angles calculated by each of the methods are shown in Table 2. It should also be noted that singularities or ambiguities exist in inverse trigonometric relations and the results at some of the steps in the calculations are appropriately chosen in the calculations. For example, $\sin^{-1}(0.5)$ has two solutions: 30^o or 150^o, but only one of them is correct. The issue can be easily resolved by comparing the solutions with those obtained at the previous sampling instant.

TABLE 2
EULER ANGLES CALCULATED USING DIFFERENT CALCULATION METHODS

	θ	ϕ	ψ
YPR	45.08	30.14	59.6
$\text{YPR}_{\text{alternate}}$	45.09	30.15	60.16
RPY	45.09	29.58	59.32
YRP	45.10	30.15	60.15
RYP	45.07	30.13	60.13
PRY	45.10	30.15	60.11
PYR	45.08	29.67	59.60

In the next case, consider that the vehicle is at the same angular position but this time it is accelerating in the x direction at the rate of 4.9m/s and the measurement a_x shows an increase of 0.5. The values measured at the sensors are shown below.

$$a_x = -0.2081 \pm 0.01 \qquad m_x = -0.4356 \pm .01$$
$$a_y = 0.3536 \pm 0.01 \qquad m_y = 0.0196 \pm 0.01$$
$$a_z = 0.6124 \pm 0.01 \qquad m_z = 0.8999 \pm 0.01$$

The Euler angles calculated from the above set of measurements based on the seven different rotation sequences are shown in Table 3 below.

TABLE 3
EULER ANGLES CALCULATED CONSIDERING THE VEHICLE IS ACCELERATING IN THE X DIRECTION

	θ	ϕ	ψ
YPR	12.01	21.25	121.34
$\text{YPR}_{\text{alternate}}$	45.09	30.15	60.16
RPY	45.42	29.58	59.32
YRP	45.10	30.15	60.15
RYP	6.95	20.93	40.43
PRY	49.36	20.41	46.88
PYR	12.01	-67.43	58.66

The above table indicates that the calculation methods which depend on the value of a_x (YPR, RYP, PRY, PYR) are affected in different ways and they all produce inconsistent

results while the methods which do not use it ($YPR_{alternate}$, RPY, YRP) remain unaffected by the failure and they all produce the correct Euler angles and these results are also consistent with each other. This pattern of the results can be used to conclude that a_x sensor is the one affected by the acceleration due to vehicle motion or that it is a failed sensor. The three consistent results also reveal the correct Euler angles. Thus the fault of one sensor does not cause the failure of the sensor system, and the system continues to give correct computation of Euler angles.

Moreover, the value of the external acceleration can be calculated using Eq. (17). This calculation is shown below.

$$\begin{aligned} e_x &= \sin\theta - \sin\hat{\theta} \\ &= \sin\left(45.09^\circ\right) - \sin\left(12.011^\circ\right) \\ &= 0.7083 - 0.2081 = 0.5002 \end{aligned}$$

The above is the value of extraneous acceleration in the x direction.

V. Conclusion

In this paper, we have presented how to utilize six rotation matrices to provide seven ways of computing Euler angles based on the six measurements by a 3-axis accelerometer and a 3-axis magnetometer. The diversified redundancy created can thus be effectively used to improve the fault tolerance of the sensor system. It also can be used to determine the extraneous field affecting it, if any.

References

[1] B. C. Chang, H. Chunlong, and M. Ilg, "Design and DSP microprocessor implementation of digital sinusoidal tracking controllers," in *Proceedings of the 2005 American Control Conference*, Portland, Oregon, 2005.

[2] M. Ilg, B. C. Chang, D. Hepner, and A. Thompson, "A micro-controller solution for AMR magnetic sensing in flying munition systems," in *Proceedings of the 2005 IEEE International Conference on Mechatronics*, Taipei, Taiwan, 2005.

[3] Honeywell, "Application Note 213: "Set/Reset Function for the Magnetic Sensors"," Honeywell Sensor Products, Solid State Electronics Center, 2002.

[4] Analog_Devices, "Data Sheet: ADXL330 Small, Low Power, 3-Axis ±3g iMEMS® Accelerometer,," 2006.

[5] MEMSIC, "Application Note: Accelerometer Fundamentals, #AN-00MX-001," 2007.

[6] T. E. Harkins and D. J. Hepner, "MAGSONDE: A Device for Making Angular Measurements on Spinning Projectiles with Magnetic Sensors," U.S. Army Research Laboratory, Aberdeen Proving Ground MD, ARL-TR-2310, January 2000.

[7] A. A. Thompson, "A Point-wise Solution for the Magnetic Field Vector," U.S. Army Research Laboratory, Aberdeen Proving Ground MD, ARL-TR-2633, January 2002.

[8] C. Chen and M. M. Trivedi, "Transformation relationships for two commonly utilized Euler angle representations," *IEEE Transactions on Systems, Man and Cybernetics,* vol. 22, pp. 555-559, 1992.

[9] B. Etkin, *Dynamics of Atmospheric Flight*: John Wiley & Sons Inc., 1972.

[10] R. Pio, "Euler angle transformations," *IEEE Transactions on Automatic Control,* vol. 11, pp. 707-715, October 1966.

[11] R. J. Patton, "Fault-tolerant Control: The 1997 situation," in *IFAC Fault Detection, Supervision and Safety of Technical Processes*, Kingston upon Hull, UK, 1997, pp. 1029-1051.

[12] N. P. Piercy, "Sensor failure estimators for detection filters," *IEEE Transactions on Automatic Control,* vol. 37, pp. 1553-1558, October 1992.

[13] K. Suyama, "Fault detection of redundant sensors and used in reliable sampled-data control systems," in *Proceedings of the 37th IEEE Conference on Decision and Control*, 1998, pp. 1161-1164.

[14] G. Gopalaratnam, C. Zorn, and A. Koch, "Multi Sensor Data fusion for Sensor Failure Detection and Health Monitoring," in *Proceddings of the 2005 AIAA Guidance, Navigation and Control Conference* San Francisco, California, 2005.

[15] J. F. G. Castellanos, S. Lesecq, N. Marchand, and J. Delamare, "A low-cost air data attitude heading reference system for the tourism airplane applications," in *2005 IEEE Sensors*, 2005.

[16] M. S. Grewal and M. Shiva, "Application of Kalman filtering to gyroless attitude determination and control system for environmental satellites," in *Proceedings of the 34th IEEE Conference on Decision and Control*, 1995, pp. 1544-1552.

[17] H. Schaub and J. L. Junkins, *Analytical Mechanics of Space Systems*: AIAA, 2003.

[18] D. Gebre-Egziabher, G. H. Elkaim, J. D. Powell, and B. W. Parkinson, "A gyro-free quaternion-based attitude determination system suitable for implementation using low cost sensors," in *The 2000 IEEE Symposium on Position Location and Navigation Symposium*, 2000, pp. 185-192.

[19] D. Gebre-Egziabher, R. C. Hayward, and J. D. Powell, "Design of multi-sensor attitude determination systems," *IEEE Transactions on Aerospace and Electronic Systems,* vol. 40, pp. 627-649, April 2004.

[20] D. Mortari and P. Singla, "Optimal Cones Intersection Technique," *Acta Astronautica* vol. 59, pp. 474-482, 2006.

[21] NGDC, "Geomagnetism, http://www.ngdc.noaa.gov/seg/geomag/geomag.shtml ", 2007.

[22] L. Wang, S. Xiong, Z. Zhou, Q. Wei, and J. Lan, "Constrained Filtering Method for MAV Attitude Determination," in *Proceedings of the IEEE Instrumentation and Measurement Technology Conference* 2005, pp. 1480-1483.

[23] S. Mobasser and S. R. Lin., "Galileo spacecraft autonomous attitude determination using a V-slit star scanner," in *1991 IEEE Aerospace Applications Conference*, 1991, pp. 1/1-12.